Current Research in Food Science 9 (2024) 100872

Contents lists available at ScienceDirect

Current Research in Food Science

journal homepage: www.sciencedirect.com/journal/current-research-in-food-science

Modeling of cooking and phase change of egg white using computational fluid dynamics

Rubén E. Sánchez-García, Orlando Castilleja-Escobedo, Rodrigo Salmón-Folgueras, José Luis López-Salinas *

Tecnologico de Monterrey, Escuela de Ingeniería y Ciencias, Ave. Eugenio Garza Sada 2501, Monterrey, N.L., 64849, Mexico

ARTICLE INFO

Handling Editor: Dr. Xing Chen

Keywords:
Food cooking
Computational fluid dynamics
CFD
phase change material
PCM
Thermal processing

ABSTRACT

This study proposes simulating the cooking of eggs by modeling fluid egg products as phase-change materials (PCMs) within a computational fluid dynamics (CFD) model. A simplified physical prototype was built to conduct experiments to tune a simpler version of the mathematical model. The information was later used to build a complete mathematical model of a real egg that was compared with experimental data. Phase transition temperature ranges, and the energy required to initialize the transition were specified. Heat transfer coefficients were estimated for both models. Experiments for thermal processing and phase change were conducted at temperatures between 90 and 100 °C. The real egg model was validated with experimental data reported elsewhere. The simulations assess the time required to cook an egg (800–1200 s), demonstrating a homogeneous increase in temperature and phase transition. However, potential overestimation in simulations was observed, likely due to differences in quantifying techniques and non-uniform cooking processes.

1. Introduction

The cooking of food is a complex process that involves key phenomena such as phase change or solidification. In cooking, this last term encompasses the process by which proteins unfold (denaturation) and then aggregate to form a solid mass (coagulation) during cooking. When an egg is exposed to heat during cooking, the proteins within the egg, including those in the albumen (egg white) and yolk, undergo significant changes. The application of heat causes these proteins to denature, meaning that their molecular structure unfolds and loses its original configuration. This process results in observable changes in texture and appearance (Luo et al., 2024). The denaturation of proteins leads to coagulation, especially in the egg white. As the protein molecules unfold, they begin to aggregate and form bonds with each other, creating a cohesive gel-like network. This network formation results in the solidification of the egg white, which becomes firm and opaque. In addition to affecting the texture, the heating process also influences the transport of species within the egg and alters its physical properties (Llave et al., 2018), (Jiang et al., 2024).

Cooking chicken eggs, due to their worldwide consumption, abundance, and nutritional benefits for the human diet, has been extensively studied (Morris et al., 2018), (Iannotti et al., 2014). Pasteurization is an important process for ensuring the microbiological safety and quality characteristics of foods. In eggs, this process occurs at a minimum temperature of 55–60 °C (Bermudez-Aguirre and Niemira, 2023), (Abbasnezhad et al., 2016). Eggs are composed of a shell, albumen or white, yolk, an air cell, and membranes (Ogura et al., 2020). However, egg white and yolk are the primary focus of most investigations. The egg white is composed of water and proteins, while the egg yolk is composed of proteins and lipoproteins and can split into granules and plasma (Razi et al., 2023), (Davari et al., 2024). Under heating, proteins undergo a denaturation and coagulation process that aggregates them and gives them a hard consistency. According to Rossi et al. (Rossi and Schiraldi, 1992), under environmental pressure conditions, the solidification of isolated egg white and yolk proteins occurs at a specific temperature range. However, lower temperatures have been reported for the denaturation of the egg whites and yolks (Abbasnezhad et al., 2015). The importance of the pasteurization process is to eliminate microorganisms that could cause serious health problems (Omar et al., 2018), (He et al., 2024). Nevertheless, these processes usually involve heating the product, which can lead to certain consequences for the egg. Proteins may be affected, and their nutritional value may also be compromised. This is

* Corresponding author. Av. Eugenio Garza Sada 2501 Sur, Col. Tecnológico; Monterrey, Nuevo León, 64849, Mexico.
E-mail addresses: Ruben.Sanchez@tec.mx (R.E. Sánchez-García), orlandocastilleja@tec.mx (O. Castilleja-Escobedo), jrsalmon@tec.mx (R. Salmón-Folgueras), jllopezs@tec.mx (J.L. López-Salinas).

https://doi.org/10.1016/j.crfs.2024.100872
Received 6 July 2024; Received in revised form 9 September 2024; Accepted 29 September 2024
Available online 1 October 2024

the reason for the use of new emerging technologies, such as high hydrostatic pressure (HHP), pulsed electric fields (PEF), pulsed light (PL), ultrasound (US), and ozonation (Agregán et al., 2023). These technologies can help minimize the impact on the food's characteristics.

Numerical methods such as finite difference, finite element, and finite volume have been used to model heat transfer in various products (Szpicer et al., 2023a), (Jenko, 2015), (Kumar et al., 2012). Other studies have been devoted to modeling the cooking of foods by specifying CFD models (Szpicer et al., 2023b), (Chhanwal et al., 2012), which consider the phase transport in porous media, phase change, changes in the structure of the materials, and diffusion of species (Khan et al., 2018). In computational simulations, a variety of thermal analyses can be performed such as temperature change, heat transfer, temperature profiles, and more (Denys et al., 2003). The coagulation process of eggs is modeled as a phase change process or phase change material (PCM), which is triggered at a given temperature, occurs throughout a temperature interval, and requires latent heat (Szpicer et al., 2023c). Computational fluid dynamics models have been specified for the study of chicken eggs for pasteurization processes in the poultry industry (Denys et al., 2004), (Denys et al., 2005), (Ramachandran et al., 2011), ventilation and humidity control in storage containers (Kumar et al., 2012), (Kumar et al., 2009), and academic capstone projects on the cooking of eggs (Galante et al., 2011).

Numerous studies have addressed the chicken egg model to simulate the internal convective streams during egg pasteurization (Jenko, 2015), (Gut et al., 2003). The physicochemical properties of different chicken egg components have been reported in different studies (Coimbra et al., 2006), (Abanikannda et al., 2007). Chicken eggs have also been subjected to analysis using various computational fluid dynamics (CFD) approaches (Wang et al., 2021), (Wang et al., 2024). The geometry of eggs has been a focal point of interest and research, leading to the development of different models (Pero et al., 2019). CFD could also validate the effectiveness of the proposed device by modeling food heating or cooking processes (Denys et al., 2003). In some of these analyses, as seen in (Ramachandran et al., 2011), an experimental pasteurization model is presented, demonstrating its viability through CFD validation. Certain analyses simplify the study by treating eggs as a unified entity (Pero et al., 2019), while others simulate the distinct components of eggs, such as yolk, white, air, and shell. Simulating all the components increases the computational time due to the refinement of the mesh at the thinner domains, such as the one representing the shell. For this reason, authors such as in (Pero et al., 2019) assumed eggs as homogeneous single-component entities with average property values. In this work, a control geometry is proposed as a physical model of the egg for experimentation. This approach allows for greater control of variables and reduces the number of factors to consider when generating the computational simulation. Consequently, the CFD model that integrates PCM can be validated. The cooking process involves a change in the state of the food, which occurs through the transition and modification of the material's properties due to the increased temperature. This demonstrates the capability of this approach to model a phase change from liquid to solid. Subsequently, A second geometry, designed to closely resemble a real egg, was created and analyzed using CFD. This geometry was then compared with previous experimental results.

2. Methodology

2.1. Materials

For greater control of the experiments and reducing external variables, as well as being able to homogenize the model over the cooking process and phase change measurements, a system with a control geometry (sphere) was used instead of real eggs. Using real eggs introduces natural factors to consider, such as the type of egg, shell thickness, porosity, yolk size, and the amount of gas trapped inside which can affect internal material movement, to obtain a homogeneous single component entity (Abanikannda et al., 2007), (Melo et al., 2021). The physical model used only egg white within a thin plastic spherical shell, a minimal amount of gas, epoxy resin, and a thermocouple. The egg white used in the experiments was obtained from a commercial brand (Claras de Huevo San Juan, Mexico). This brand provides pasteurized liquid egg whites, ensuring food safety. The spherical shells used in the experiments were standard ping-pong balls. These spheres were made of PVC material, ensuring their durability and suitability for the experimental setup. They had a mean diameter of 40 mm and a wall thickness of 2 mm.

Using the control-physical model, the experiments were conducted with enhanced precision in setting the variables under study. This methodological approach facilitated improved visualization and more accurate measurement of both the cooking and phase change processes. Consequently, it enabled a more focused analysis and rigorous comparison of the experimental outcomes, thereby enhancing the depth and reliability of our findings.

2.2. Experimental setup and measurements

2.2.1. Thermal processing

The experimental cooking (EC) nomenclature was employed for the temperature measurement process. The following steps were followed: (I) Weighing the sphere: the sphere was weighed employ an electronic balance; (II) Creating a hole in the sphere: a hole was generated in the sphere, which served as an entry point for injecting egg white, subsequently, the same aperture was used for inserting the thermocouple; (III) Injecting egg white: egg white was injected into the sphere until it reached a saturated state with an average mass of 30 g and a variation of 1.19 g; (IV) Inserting a thermocouple: a thermocouple connected to a digital thermometer was carefully placed in the center of the sphere; (V) Sealing the sphere: the hole in the sphere was covered with epoxy resin or any suitable material; (VI) Heating water: approximately 2 L of water was heated in a beaker or a suitable container. The temperature of the heating water bath was set to three different values for the experiment, A = 90 °C, B = 95 °C, C = 100 °C, the temperature was monitored with an alcohol thermometer; (VII) Placing the sphere in heating water: the prepared sphere was then placed in hot water. The cooking time was determined based on factors such as the desired internal temperature to be reached and the reference values for the cooking of the egg for human consumption (Omar et al., 2018). This time was chosen to avoid overcooking or burning the egg white (Shahbaz et al., 2018). (VIII) Measuring temperature vs. time: throughout the cooking process, the temperature inside the sphere was measured using a type K thermocouple and a digital thermometer. The experimental setup is shown in Fig. 1. These temperature readings were recorded to create a plot of the temperature as a function of time, allowing for a visual representation of the cooking progress. By adhering to this standardized and controlled methodology, the experiments were executed consistently, ensuring uniform conditions to compare experiments.

2.2.2. Relative phase abundance

The phase change (PC) nomenclature was implemented for the phase change process. The following steps were conducted: (I) The procedure closely resembles thermal processing, with the distinction that a thermocouple was not inserted; (II) The sample was thermally treated during a specific timespan (60–500 s) (Llave et al., 2018), (Pero et al., 2019); (III) Removing the sphere: after the selected time had elapsed, the sphere was removed from the water; (IV) Cut the sphere: the sphere was carefully cut to extract the remaining liquid; (V) Weighing the phases: the liquid phase and solid phase materials were individually weighed; (VI) Calculating phase fraction: the fraction of each phase (liquid and solid) was determined by comparing their weights to the initial weight of the injected egg white. This calculation provides valuable information about the extent of phase change and the distribution of phases within the physical model.

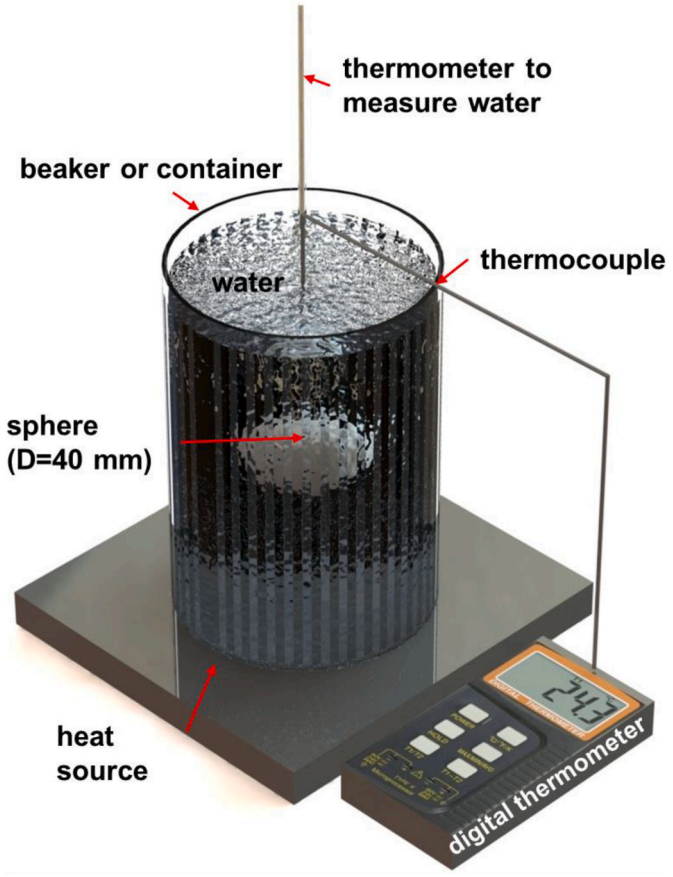

Fig. 1. Experimental setup.

2.3. Computational fluid dynamics model

CFD software is essential in engineering and scientific analysis for the efficient solution of partial differential equations (PDEs). These equations govern fluid flow phenomena and more, and there are three primary numerical methods employed for their solution. The finite difference method (FDM) discretizes the classical form of the PDE, while the finite element method (FEM) discretizes the weak form, and the finite volume method (FVM) discretizes the conservation form. Among these methods, FVM stands out for its mathematical simplicity, particularly when compared to some of the more complex variants of FEM (Wu et al., 2022). Moreover, FVM excels in scenarios where the conservation of quantities is crucial, making it the preferred choice for simulating various engineering problems that require accurate preservation of conserved quantities. In the analysis, ANSYS® Fluent software was used, which implements the Green-Gauss finite volume method with a cell-centered formulation (Moukalled et al., 2016). This choice of software is particularly suitable for our simulations due to its robust capabilities in accurately solving conservation equations and its user-friendly interface, facilitating efficient setup and analysis of complex fluid flow problems.

For the simulations, the geometries were sketched using ANSYS® SpaceClaim, and the mesh was created in ANSYS® Mechanical. The specification of the model and visualization of the results were conducted in ANSYS® Fluent. The software employs algorithms specifically designed to represent the behavior of fluid flow, including conservation equations for mass, energy, and momentum within a defined domain (Table 1). These equations are coupled with the model to accurately represent the momentum and heat transfer occurring within the system.

Table 1
Equations used in the analysis, description, and variables.

Conservation equations	Equation	ID
Continuity equation	$\frac{\partial \rho}{\partial t} + \nabla \cdot (\rho \vec{v}) = S_m$	(1)
Conservation of momentum	$\frac{\partial}{\partial t}(\rho \vec{v}) + \nabla \cdot (\rho \vec{v} \vec{v}) = -\nabla p + \nabla \cdot (\bar{\bar{\tau}}) + \rho \vec{g} + \vec{F}$	(2)
Conservation of energy	$\frac{\partial}{\partial t}\left(\rho\left(e + \frac{v^2}{2}\right)\right) + \nabla \cdot \left(\rho v \left(h + \frac{v^2}{2}\right)\right) = \nabla \cdot \left(k \nabla T - \sum_j h_j \vec{J_j} + \bar{\bar{\tau}} \cdot \vec{v}\right) + S_h$	(3)
Enthalpy	$H = h + \Delta H$	(4)
Sensible enthalpy	$h = h_{ref} + \int_{T_{ref}}^{T} C_p dT$	(5)
Liquid fraction	$\beta = \frac{T - T_{solidus}}{T_{liquidus} - T_{solidus}}$ *if* $T_{solidus} < T < T_{liquidus}$ $\beta = 0$ *if* $T < T_{solidus}$ $\beta = 1$ *if* $T > T_{liquidus}$	(6)
Solid Fraction	$\Phi_S = 1 - \beta$	(7)
Energy equation for PCM problems	$\frac{\partial}{\partial t}(\rho H) + \nabla \cdot (\rho \vec{v} H) = \nabla \cdot (k \nabla T) + S$	(8)
Density	$\rho = \rho_0 + \rho_1 T$	(9)
Thermal conductivity	$k = k_0 + k_1 T$	(10)
Specific heat	$c_p = c_{p0} + c_{p1} T$	(11)
Rayleigh number	$Ra_D = \frac{g D^3 \beta_v (T_s - T_\infty)}{\nu \alpha}$	(12)
Nusselt number	$\overline{Nu}_D = \frac{\overline{h} D}{k}$	(13)
	$D = 2\left(\frac{3V_{egg}}{4\pi}\right)^{1/3}$	(14)
Churchill correlation	$\overline{Nu}_D = 2 + \frac{0.589 Ra_D^{0.25}}{\left[1 + \left(\frac{0.469}{Pr}\right)^{9/6}\right]}$ For $Pr > 0.5$ and $Ra_D < 1 \times 10^{11}$	(15)

2.3.1. Geometry

The geometry of the sphere, set at the center of the drawing plane with a diameter of 40 mm, was a solid piece or a single volume. The resulting geometry is illustrated in Fig. 2.

2.3.2. Mesh and mesh independence test

The mesh serves as a discretization of the domain or volume, enabling the representation of the physical system in a numerical form. This is why meshing is crucial for numerical simulations and calculations. The volume is divided into small sub-volumes or elements. The mesh was created using the mechanical mesh tool with the physics preference of CFD and the solver preference of Fluent. The element order was specified as linear, and the mesh type included both tetrahedral and hexahedral elements. To ensure the quality and viability of the mesh, a mesh independence test was performed to ensure that the simulation results were not influenced by the number of elements. Four refinement levels were evaluated: 40000, 110000, 260000, and 350000 elements (Fig. 3). The parameter that was studied was the average temperature of the volume that the model reached at 10 s from the beginning.

By conducting a mesh independence test, it was determined that employing a mesh comprising approximately 260,000 elements was the most appropriate. Using a finer mesh would not affect the accuracy of the results and would significantly increase computational time. The properties of the mesh in the model are detailed in Table 2, and the mesh distribution within the geometry is shown in Fig. 4.

2.3.3. Initial and boundary conditions

The Fluent solver was configured as pressure-based, and the analysis was set to transient. Models were specified for energy (equations (3)–(5)) and phase change (equations (7)–(9)). The initial value of the temperature was specified at 25 °C. Materials were defined with properties and parameters for the egg white and the spherical shell. The properties used in the analysis are outlined in Table 3 (Bermudez-Aguirre and Niemira, 2023), (Jenko, 2015), (Moukalled

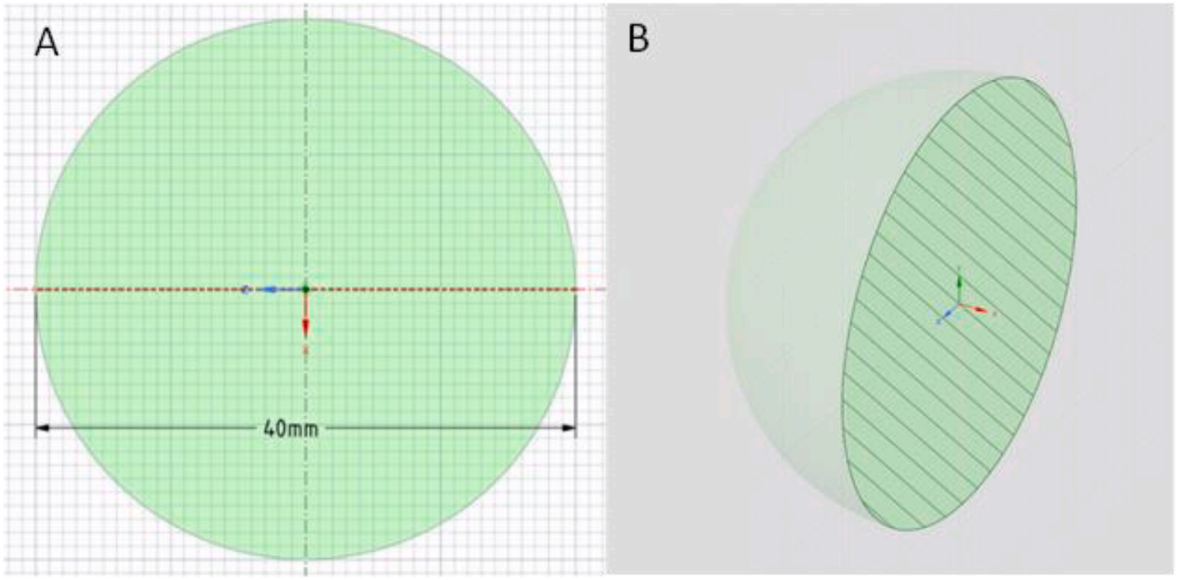

Fig. 2. (**A**) Sketch of the sphere; (**B**) section view of the geometry in the drawing tool.

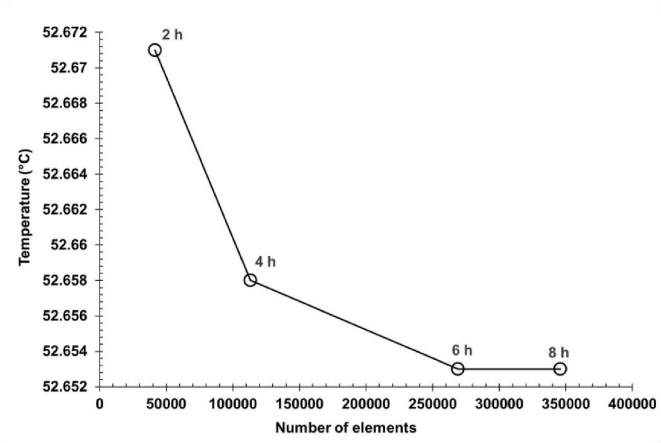

Fig. 3. Mesh independence test of the variable of volume average of the temperature at 10 s.

Table 2
Mesh properties for the geometry.

Geometry	Element size (m)	Nodes	Elements
Sphere	7e-4	50310	268009

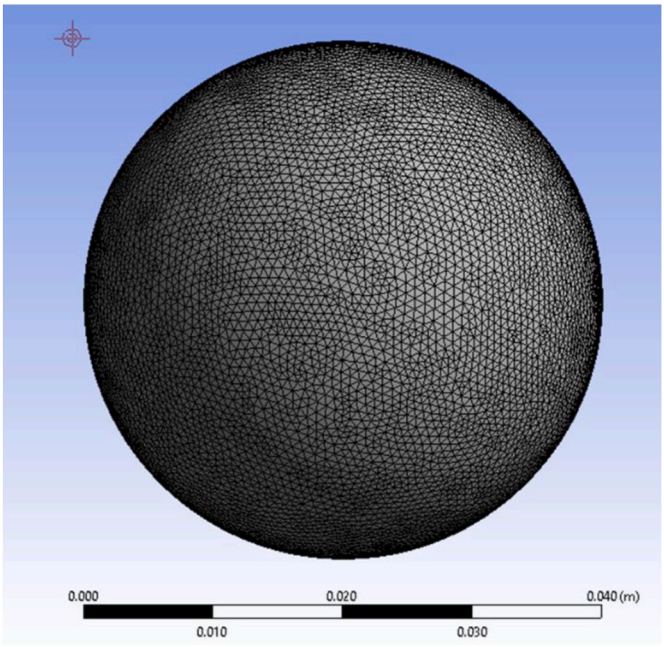

Fig. 4. Mesh distribution in the geometry.

et al., 2016). To effectively simulate the thermal processing and the phase change, properties were expressed using polynomial functions (equations (10)–(12)). This enables the visualization of how properties change over time in response to temperature (Denys et al., 2005), (Atilgan and Unluturk, 2008). The cooking processes for the simulation were modeled using a PCM approach, with data for the egg white provided in Table 4. One domain is considered for discretization, the egg white, and one interface or wall, the shell (i.e. the egg white domain is modeled with distributed-parameters system, while the shell is formulated as thermal resistance). The model is assumed to be surrounded by water, so a convective condition is defined at the wall surface. The wall thickness was set as 2 mm. The free-stream temperatures were those discussed in the experimental section (90 °C, 95 °C, 100 °C), and the heat transfer coefficient was specified as 2144 W m^{-2}·K^{-1}. To determine the heat transfer coefficient, a free convection correlation for a spherical geometry was used (equations (12)–(15)), (Rodríguez Maestre et al., 2021), (Nellis and Klein, 2009). The transient model was simulated for up to 800 s.

3. Results and discussion

3.1. Experimental results

3.1.1. Thermal processing

The temperature measurements within the physical model are displayed in Fig. 5. Conducting the experiments not only allows us to compare these data with the simulated data to validate the CFD model, but also to verify the behavior of the proposed physical model. The plot displays the mean values of the cases studied, with error bars

Table 3
Thermal properties of the polynomial profile of egg white and spherical shell.

Egg Components	Density [ρ]		Thermal conductivity [k]		Specific heat capacity [c_p]	
	ρ_0 [kg·m^{-3}]	ρ_1 [kg·m^{-3}K^{-1}]	k_0 [W·m^{-1}·K^{-1}]	k_1 [W·m^{-1}·K^{-1}]	$c_{p,0}$ [J·kg^{-1}·K^{-1}]	$c_{p,1}$ [J·kg^{-1}·K^{-1}]
White	1133.19	−0.06	0.390	4.1	2629.05	2.39
Shell	1300	–	0.16	–	900	–

Table 4
Thermodynamic parameters for egg PCM.

Process	Phase 1	Phase 2	Phase change temperature (1–2) [K]	Transition interval (1–2) [K]	Latent heat [kJ kg^{-1}]
White solidification	Liquid white	Solid white	336.15	3	12.2

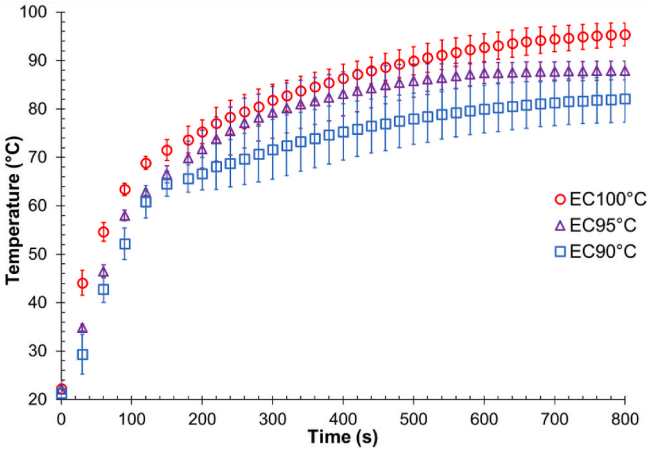

Fig. 5. Temperature measured at the center of the physical model as a function of time at different heating water temperatures.

representing the standard deviation based on experiments conducted with at least 5 replicates for each scenario.

3.1.2. Relative phase abundance

To evaluate phase transition (i.e., solidification: the process of transforming a substance from a fluid phase to a solid phase. In the context of cooking, solidification commonly refers to the coagulation of proteins, such as the denaturation and subsequent aggregation of proteins in eggs during cooking, leading to the formation of a solid mass). The solid fraction was chosen as a parameter to construct the plot shown in Fig. 6, where the error bars were obtained with at least three replicates. The initial phase is the liquid form of the egg white, while the fully cooked form represents the solid form phase (Φ_S). By analyzing the solid fraction, the transformation of egg white from its initial liquid state to its final solid state during the cooking process can be tracked. This plot provides valuable insights into the progression of phase change and helps us understand the degree of completion or the time required for the solid fraction to reach a certain level. The use of the solid fraction as a measure enables a clearer understanding of the transformation occurring within egg white. It provides a quantitative representation of the phase change process and facilitates the comparison of different cooking scenarios or conditions.

It is important to clarify that an opportunity to reduce costs and energy expenses exists (Szpicer et al., 2023b). Typically, the reference point for cooking an egg is when the water reaches its boiling point, which can take between 5 and 10 min. Adding the time required for the egg to cook, which is another 10–15 min, results in a total energy/fuel consumption range of 20–30 min. However, through a review of the literature and experiments, it was observed that the minimum phase/-cooking change for human consumption begins at 150–200 s or when

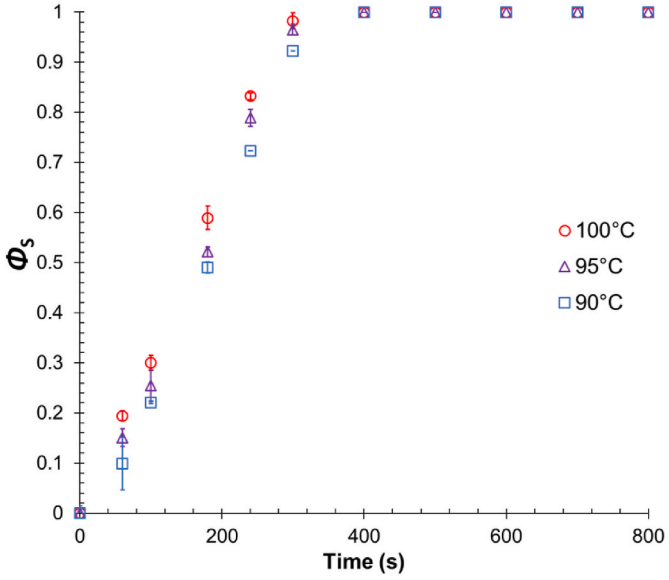

Fig. 6. Egg white solid fraction (Φ_S) as a function of time at different heating water temperatures.

the temperature reaches 60–65 °C (Bermudez-Aguirre and Niemira, 2023), (Omar et al., 2018). This indicates that waiting for the water to reach boiling is not necessary; instead, the time should be considered starting from the beginning of heating, potentially reducing the total cooking time by 3–5 min. While this may not significantly impact small-scale cooking, it can lead to substantial savings on a larger or industrial scale. Additionally, this consideration does not account for the positive environmental impact, such as reduced energy, fuel, or water consumption, resulting in significant savings and a reduced carbon footprint.

3.2. Computational simulation results

3.2.1. CFD temperatures

In the thermal processing simulations (S), the internal temperature of the sphere was monitored and recorded throughout the cooking process. This allowed for a comprehensive understanding of how the temperature evolved, providing insights into the heating behavior and the progression of cooking (Fig. 7).

3.2.2. CFD phase change

The phase change indicates cooking progress as egg white transitions from its initial liquid to a solid phase. The percentage of liquid was measured as a volume-average, which served as a measure to quantify the phase change extent (Fig. 8).

In material sciences, a PCM is a material that stores a large amount of

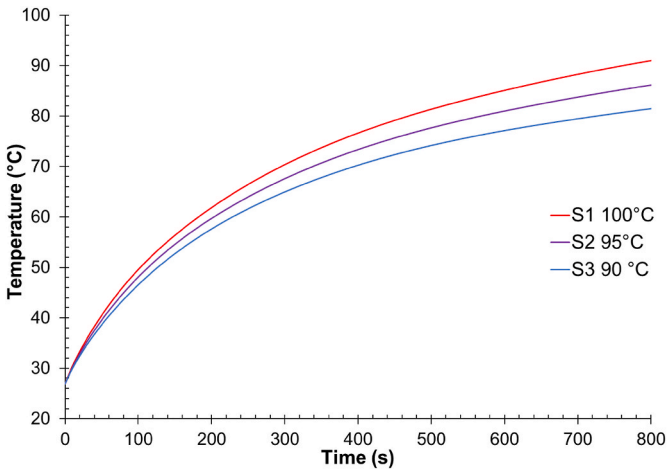

Fig. 7. Volume-averaged temperature profile in the egg white CFD model over time at different heating temperatures.

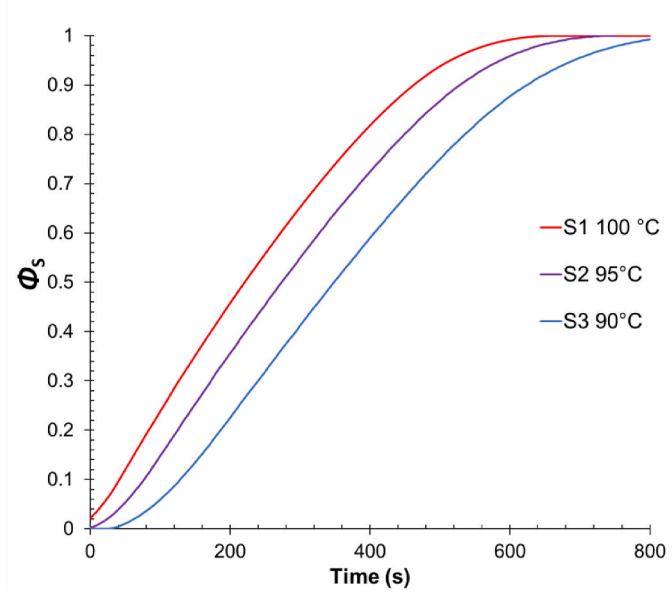

Fig. 8. Phase change profile that represents changes in the liquid fraction to solid fraction during the cooking process.

energy as latent heat. Commercial CFD software, such as ANSYS® Fluent, includes phase change modeling features that allow the simulation of this type of processes. Some studies have focused on defining the optimal thermal conditions for pasteurization without reaching the phase change (Szpicer et al., 2023b). However, it is important to note that certain limitations arise when simulating the phase change process. The current CFD model is primarily developed to manage pure materials, alloys, and mixtures. In contrast, egg white is a complex mixture containing proteins, fat, ash, and other components (Coimbra et al., 2006). This complexity should be considered when interpreting the results of the experimental part. Although the model may not perfectly capture all the intricacies of egg white composition (Jiang et al., 2024), (Liu et al., 2024), it still provides valuable insights and predictions. The combination of monitoring the internal temperature and analyzing the phase change allowed a comprehensive evaluation of the cooking process. It provided information on the relationship between temperature and phase transition, allowing a better understanding of the thermal behavior and cooking kinetics of the egg. Under this assumption, the materials change their phase and their characteristic physicochemical properties in a certain temperature range based on a specific temperature threshold (Abbasnezhad et al., 2016), (Wang et al., 2021). This phase change requires latent heat for the transformation process to occur (Pero et al., 2019).

3.3. Comparison experimental vs CFD simulation

Figs. 9 and 10 show the comparison of the experimental and simulated egg white temperature and solid phase relative abundance as a function of time under different heating fluid temperature. A comparison of the experimental measurement and the CFD model is presented in Fig. 9, for the thermal processing and Fig. 10 for the phase change (solidification). Fig. 9 shows a close agreement between the experimental and simulated temperature profiles. However, slight variations in the alignment of the experimental data with the simulation are observed, mainly attributable to differences in the position of the temperature measurement probe. In the experiment, the thermocouple was placed at the central point of the physical model, while in the simulation, the volume-averaged temperature was determined over the entire egg white domain. A similar behavior was reported in (Wang et al., 2021), (Pero et al., 2019). From Fig. 9, it is highlighted that the thermal behavior of the physical model can be accurately predicted by the simulation model. This is relevant considering that the egg white phase transition process along with conduction and convection heat transfer mechanisms are involved.

Regarding the relative abundance of the egg white solid phase, it can be intuitively expected that higher solidification degrees will be achieved with higher heating fluid temperatures, as shown in Fig. 10. However, Fig. 10 reveals a slight difference between the experimentally determined and numerically predicted solid-phase relative abundance history. In this case, the solid-phase relative abundance was underestimated by the CFD simulation model under all three heating fluid temperatures tested. This can be justified based on the experimental approach used to quantify the solid phase fraction in the physical model. During the solidification process of egg white, a continuous network is generated due to the aggregation of proteins, which gives a hard consistency to this egg product (Ferry, 1948). This network encloses a certain amount of liquid egg white, which is finally quantified within the egg white solid fraction. Therefore, the experimentally measured egg white solid fraction could be expected to be higher than numerically predicted. From the simulation data, it is observed that the solidification process of the egg white occurs uniformly from the outer surface of the sphere towards the center. However, in the experiments the cooking process is governed by the heterogeneity of the egg white (Razi et al.,

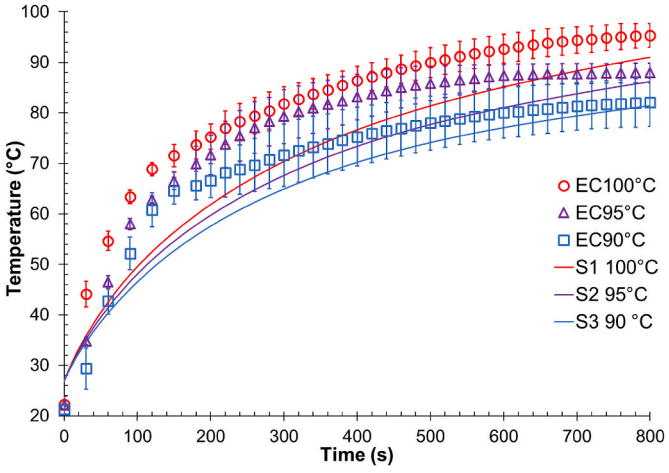

Fig. 9. Temperature of the physical and simulated (volume-averaged) spherical models under different heating fluid temperatures. For the physical model, temperature was measured at the center of the sphere.

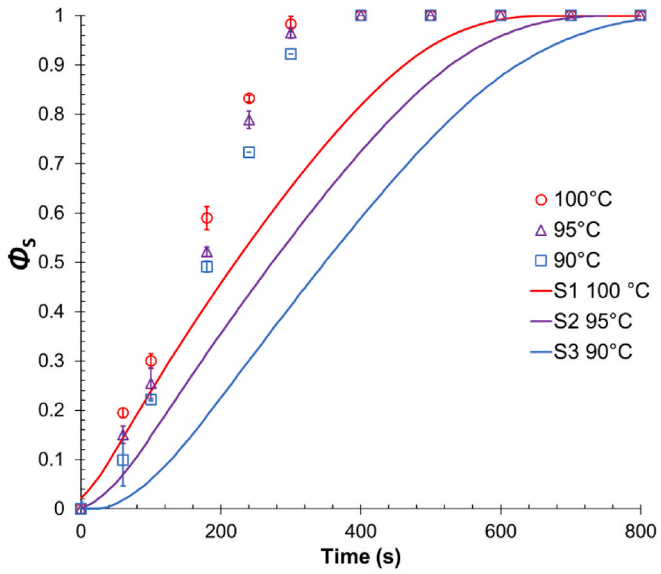

Fig. 10. Volume-averaged temperature of the solid-phase relative abundance in experimental and simulated egg white models under different heating fluid.

2023). In other words, even that there is a geometric order in the solidification, this is not fully homogenous, resulting in areas where liquid becomes trapped within the solid.

Based on the experimental validation of the simulation model, a second model was generated to predict the behavior thermal behavior of an authentic egg. This model includes the egg white and egg yolk domains (Fig. 11), where the egg shape was delineated according to data provided elsewhere (Kruenti et al., 2022), (Grunden et al., 1975). The eggshell was specified as a thermal resistance within the mathematical model; thus, no geometrical subdomain was represented. The mesh features are summarized in Table 5 and are shown in Fig. 12. It was determined that for this scenario, which involves multiple domains and an interface between them, a mesh with a larger number of elements is required to obtain a better response.

The specified thermal properties and the thermodynamic parameters of the egg components governing these reactions were obtained from the literature and are provided in Table 6 (Jenko, 2015), (Moukalled et al.,

Table 5
Mesh properties of the geometries.

Geometry	Element size (m)	Nodes	Elements
Egg white	5.75e-4	161087	862667
Egg yolk	5.75e-4	15453	80153

2016). As shown in Table 7, solidification occurs at different temperature intervals for the egg yolk and the egg white components. The liquid phase was within the temperature range from 0 °C to 60 °C, while the solid phase begins within the temperature range of 60 °C–65 °C (Wang et al., 2021), (Shahbaz et al., 2018). The initial value of the temperature of the egg domain was set at 25 °C. The egg is assumed to be surrounded by water. However, no water domain is simulated. Instead, a convection condition was specified on the outer surface boundary of the egg geometry to simulate the heat exchange process. The wall thickness (eggshell) was set as 0.3 mm as reported in (Yamak et al., 2016). The free-stream temperature was specified at 95 °C, and the heat transfer coefficient was specified as 2144 W $m^{-2}{\cdot}K^{-1}$ as a free convection correlation (equations (12)–(15)) (Rodríguez et al., 2021), (Nellis and Klein, 2009). The transient model was simulated for up to 2000 s. For the simulations, the Egg Simulation (ES) was used to explore several scenarios, providing insights into the temperature distribution over time within the egg domain and the phase transition from liquid to solid phase. According to (Omar et al., 2018), the egg is expected to be fully cooked and ready for human consumption approximately 1200 s after the start of the process.

Fig. 13 illustrates the thermal distribution within the egg domain, displaying a homogeneous heating process from the outer wall to the center egg similar to the case of study in (Wang et al., 2021), (Wang et al., 2024), (Pero et al., 2019). In Fig. 14, the transition from liquid to solid phase of the egg is show, highlighting the visible phase change process within both the white and yolk domains. Furthermore, Fig. 15 demonstrates the evolution of temperature distribution and phase change within the egg under different water heating scenarios (75 °C–105 °C).

Fig. 16 shows different scenarios of egg cooking from different research works, with the aim of comparing the simulations obtained from the egg model (i.e., the egg-like CFD model) to experimental data. The measurement of the temperature was done in the egg yolk. The difference in the experimental data is due to a heterogeneity in the materials and initial temperatures in each research work. As mentioned

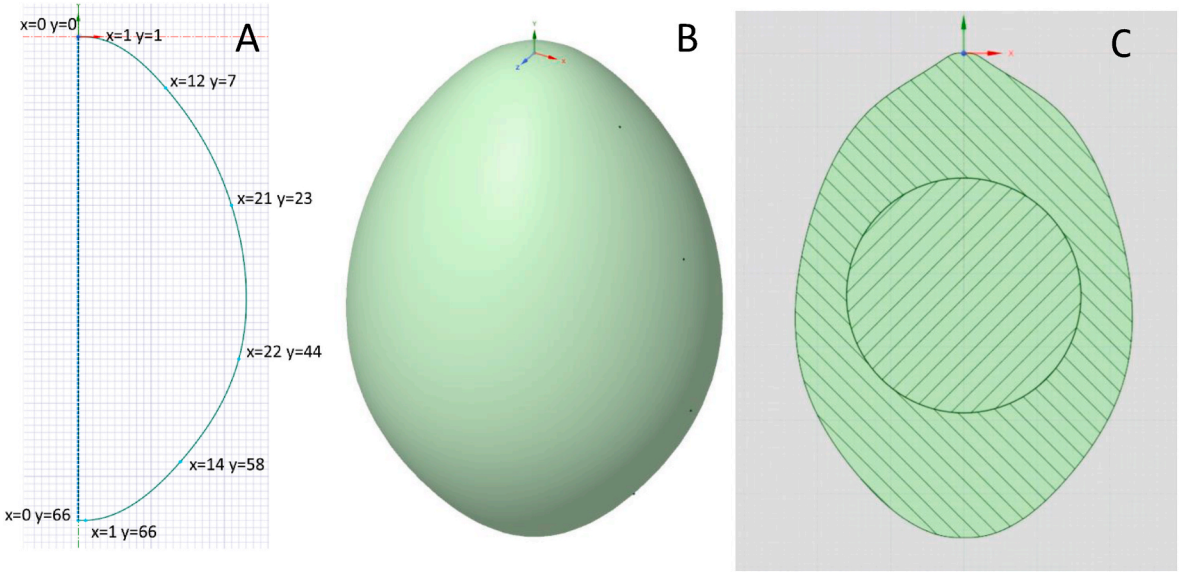

Fig. 11. (**A**) Egg point creation; (**B**) geometry of the egg model; (**C**) section view of the egg model.

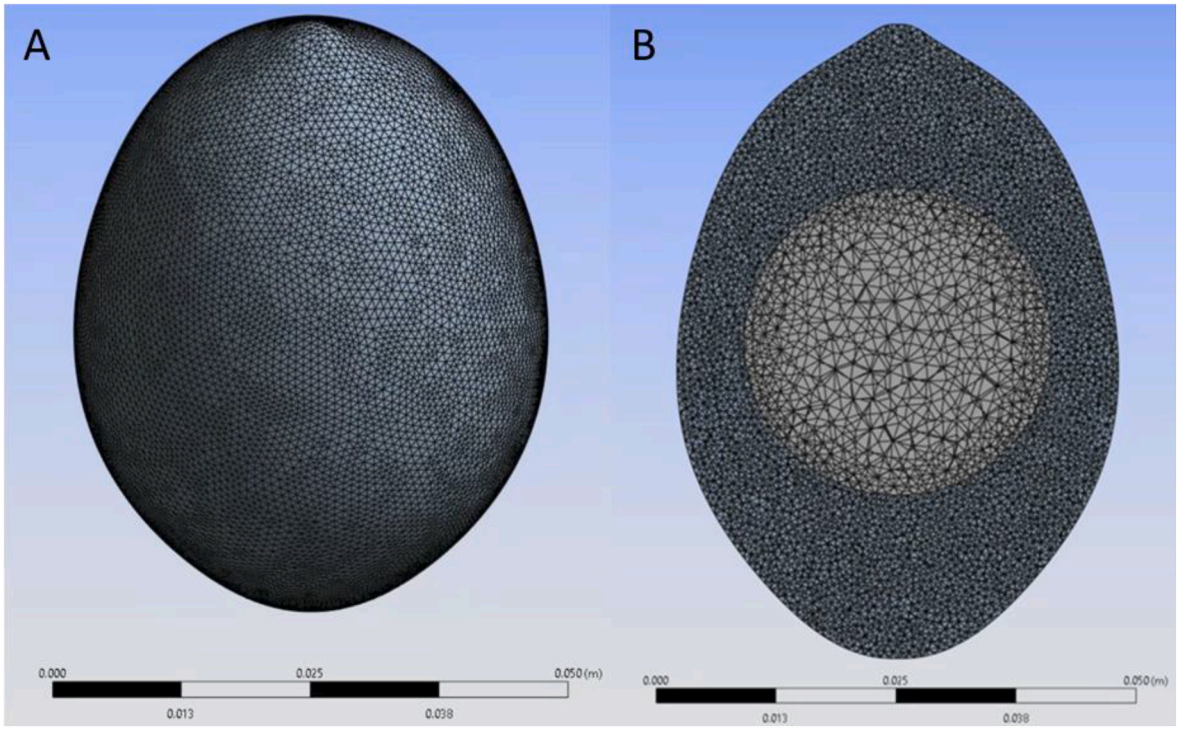

Fig. 12. (**A**) Mesh for the egg model; (**B**) Section view for the egg showing the egg white and yolk.

Table 6
Thermal properties of the domains (Jenko, 2015), (Moukalled et al., 2016).

Domain	Density [kg m^{-3}]	Thermal conductivity [W m^{-1} K^{-1}]	Heat capacity c_p (J kg^{-1} K^{-1})
Egg liquid yolk	1100	0.31	3700
Egg liquid white	1134	0.48	3800
Egg solid yolk	1032	0.34	2700
Egg solid white	1100	0.40	3700
Egg shell	2300	2.25	888

in the work of Chantarapanont et al. (2000), the curve departs from the trend of the others, since its cooking process does not begin at room temperature conditions, but rather a lower temperature in a range of 10–21 °C. Also, the use of larger eggs which, due to the greater amount of material, takes longer to cook. Despite those observations, a close correlation is observed between the simulated data and the experimentally measured values reported elsewhere (Chantarapanont et al., 2000), (Grijspeerdt and Herman, 2003), (Minéia et al., 2005). This gives confidence to use the proposed CFD model to predict different cooking scenarios.

4. Conclusions

In this study, the cooking process of a hard-boiled egg was proposed to be simulated by treating the fluid egg products as a phase-change material (PCM). This involved creating a control geometry as a physical model of the egg white, as well as a model that represents the geometry of a real egg. This approach enabled the specification of a computational fluid dynamics (CFD) model using PCM mathematical models to predict the transition from fluid to solid phases and to track the fluid and solid fractions. Control experimental measurements from a physical model were compared to mathematical model. The objective of these experiments was to verify whether representing the cooking process as a phase-change material system could accurately predict the temperature and evolution of phase changes over time. For the parameters needed for the mathematical model, the physical and transport properties of the simulated egg products (e.g., density, thermal conductivity, specific heat capacity, viscosity, activation latent energy, phase-transition temperature range, etc.) were screened from the literature. The temperature dependence of these properties was considered in the model. The characteristics of the domain, eggshell thickness, geometry dimensions, and volumes of egg white and yolk were obtained from the literature. To validate the CFD model, a set of control experiments was designed to minimize variability posed by real chicken eggs. An estimation of the heat transfer coefficient was conducted for both the physical model and the real egg model, assuming a control volume surrounded by hot water. Additionally, determination, measurement, and comparison of the solid fraction (i.e., the hard-boiled egg fraction) were performed. The experimental results showed consistent behavior across different study scenarios, evident in both temperature profiles and phase changes. In the phase-change experiments, non-uniform behavior in the transition of states was observed, which stemmed from the random initiation of the process within the material. The simulation results confirmed that the time needed to cook an egg or boil it, between 800 and 1200 s, coincided with the findings of previous studies. Moreover, a uniform increase in temperature within the

Table 7
Thermodynamic parameters for egg solidification processes (Wang et al., 2021), (Shahbaz et al., 2018).

Process	Phase 1	Phase 2	Phase change temperature (1–2) [K]	Transition interval (1–2) [K]	Latent heat [kJ kg^{-1}]
Yolk solidification	Egg yolk	Solid yolk	343.15	3	12.2
White solidification	Egg white	Solid white	336.15	3	12.2

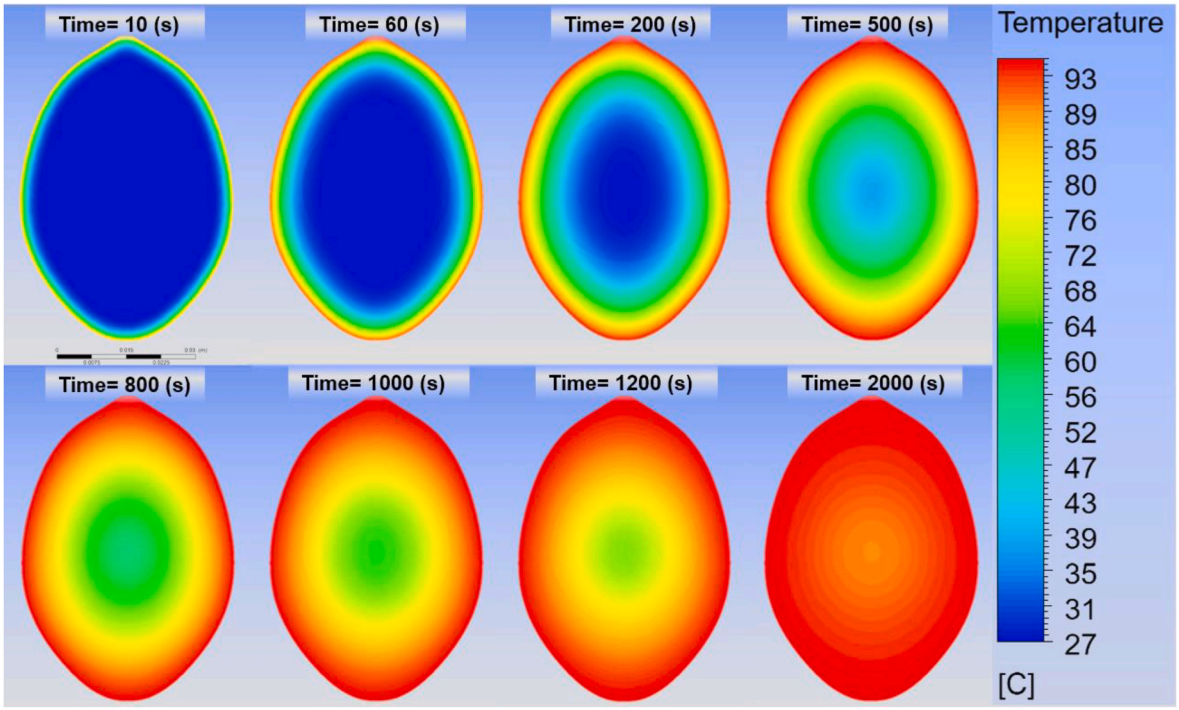

Fig. 13. Temperature profile inside the egg model at different time frames.

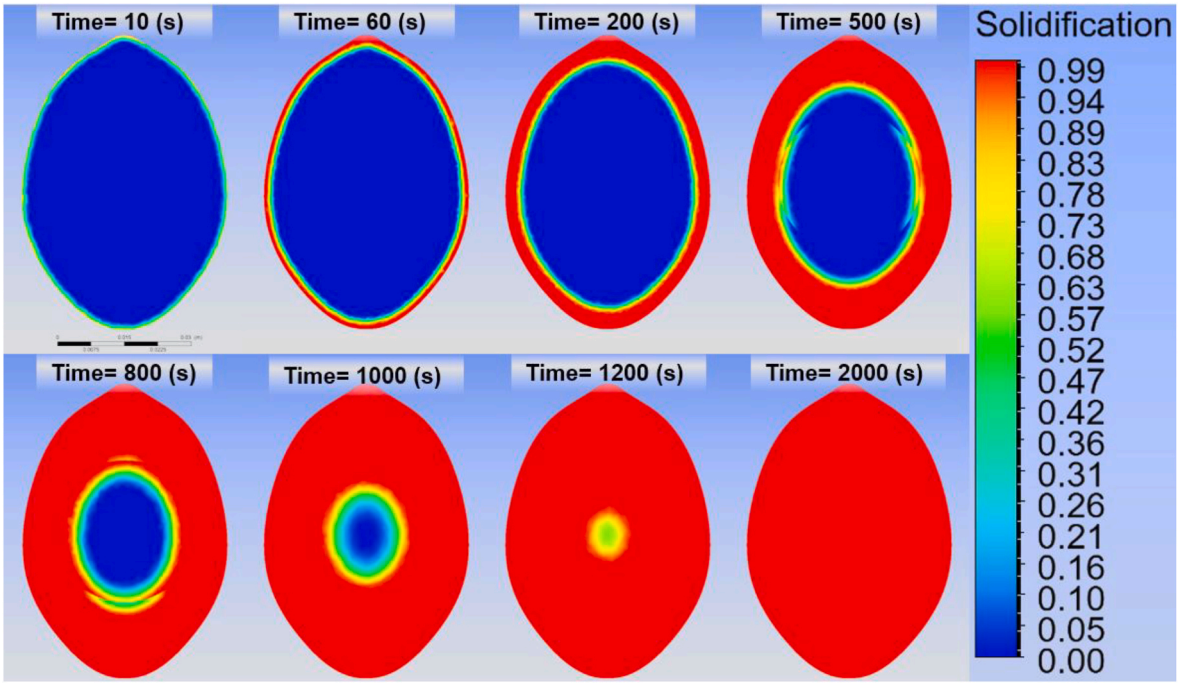

Fig. 14. Phase change of the egg white and yolk (solidification) at different time frames.

simulated egg product was noted, progressing evenly from the outer wall toward the center of the model volume. The phase transition front initiated from the outer wall and propagated homogeneously toward the center of the model. Strong agreement was observed between the experimental and simulated temperature profile data. However, the temperatures and phase transitions obtained from the simulation may have been overestimated. This discrepancy could be attributed to differences in the measurement process: while the thermal transition experiments measured a point within the physical model, the CFD utilized a volume averaged. Additionally, the solidification process of a hard-boiled egg may occur heterogeneously, potentially retaining some liquid material encapsulated within the solid continuous phase, in contrast to the homogeneous form predicted in the CFD model. The model of the real egg showed good alignment with the temperature profile compared to previous experimental studies reported elsewhere. Based on the findings from the physical control model, a complete egg model including the egg white, yolk, and eggshell was specified using ANSYS® Fluent. A close correlation was observed between the

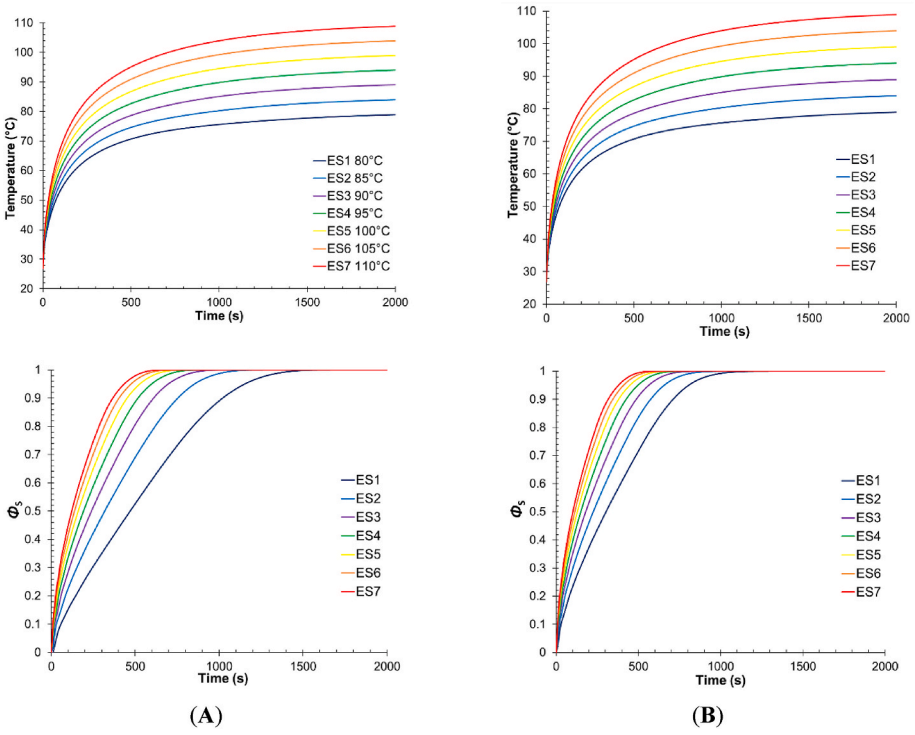

Fig. 15. Temperature and phase change profiles under different heating scenarios; (A) egg white; (B) egg yolk.

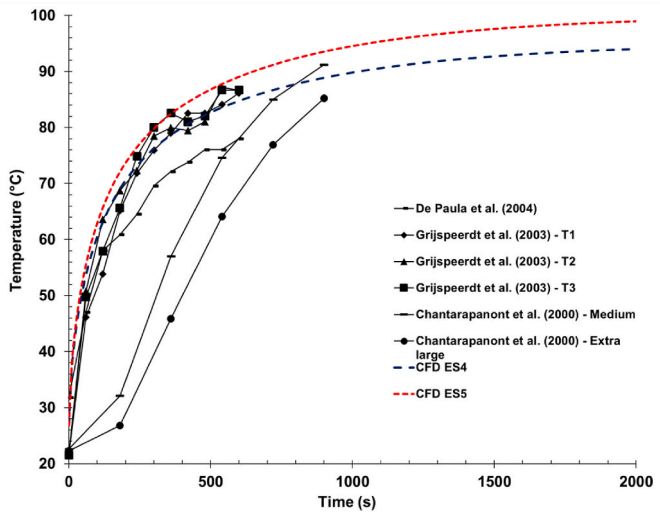

Fig. 16. Temperature comparison of the egg yolk in different studies vs. the simulation obtained by CFD ANSYS® Fluent (Chantarapanont et al., 2000), (Grijspeerdt and Herman, 2003), (Minéia et al., 2005).

simulated temperature profile and the experimental data reported elsewhere. Some discrepancies were observed among different experimental datasets reported in the literature, which have been attributed by some authors to differences in egg size, geometry, shell color, initial temperature, among others. Differences in experimental conditions may also contribute to these discrepancies in some of the temperature profiles compared in this work.

Author contributions

The manuscript was written through the contributions of all the authors. All authors have approved the final version of the manuscript.

CRediT authorship contribution statement

Rubén E. Sánchez-García: Conceptualization, Methodology, Software, Formal Analysis, Investigation, Writing–original draft, Writing–Review & Editing. **Orlando Castilleja-Escobedo:** Conceptualization, Methodology, Software, Investigation, Writing–Review & Editing. **Rodrigo Salmón-Folgueras:** Supervision, Conceptualization. **Jose Luis Lopez-Salinas:** Conceptualization, Methodology, Software, Resources, Writing–Review & Editing, Supervision, Project Administration.

Funding

This research did not receive any specific grant from funding agencies in the public, commercial, or not-for-profit sectors.

Declaration of competing interest

The authors declare that they have no known competing financial interests or personal relationships that could have appeared to influence the work reported in this paper.

Data availability

Data will be made available on request.

Acknowledgments

R.E.S.-G. gratefully acknowledge the Ph.D. scholarship received through the Mexican National Council for Humanities, Science and Technology, Mexico https://conahcyt.mx/ as well as the support from Tecnológico de Monterrey through a graduate scholarship. The authors acknowledge financial support from Tecnológico de Monterrey, Campus Monterrey.

Nomenclature

Cp	Specific heat capacity [$J{\cdot}kg^{-1}{\cdot}K^{-1}$]
D	Diameter of the sphere [m]
$\vec{F}$	Gravitational body force and external body forces [$m{\cdot}s^{-2}$]
g	Gravity acceleration (scalar) [$m{\cdot}s^{-2}$]
$\vec{g}$	Gravity acceleration [$m{\cdot}s^{-2}$]
H	Enthalpy [$J{\cdot}kg^{-1}$]
ΔH	Latent enthalpy [$J{\cdot}kg^{-1}$]
h	Sensible enthalpy [$J{\cdot}kg^{-1}$]
$\overline{h}$	Heat transfer coefficient [$W{\cdot}m^{-2}{\cdot}K^{-1}$]
h_j	Formation enthalpy [$J{\cdot}mol^{-1}$]
h_{ref}	Reference enthalpy [$J{\cdot}kg^{-1}$]
I	Unit tensor [Pa]
$\vec{J_j}$	Diffusion flux of species [$mol{\cdot}m^{-2}{\cdot}s^{-1}$]
k	Thermal conductivity [$W{\cdot}m^{-1}{\cdot}K^{-1}$]
k_{eff}	Effective conductivity [$W{\cdot}m^{-1}{\cdot}K^{-1}$]
p	Static pressure [Pa]
S_h	Volumetric heat sources [$W{\cdot}m^{-3}$]
S_m	Source term
T	Temperature [K]
T_{ref}	Reference Temperature [K]
T_s	Temperature at the surface [K]
T_∞	Bulk temperature of the fluid [K]
$x_0 + x_1 T$	Coefficients of polynomial correlation
$\vec{v}$	Velocity of the fluid [$m{\cdot}s^{-1}$]
α	Thermal diffusivity [$m^2{\cdot}s^{-1}$]
β_v	Volumetric thermal expansion coefficient [K^{-1}]
μ	Molecular viscosity [Pa·s]
ρ	Density of the fluid [$kg{\cdot}m^{-3}$]
$\overline{\overline{\tau}}$	Shear stress tensor [Pa] $\overline{\overline{\tau}} = \mu\left[(\nabla\vec{v} + \vec{v}^T) - \frac{2}{3}\nabla\cdot\vec{v}I\right]$
ν	Kinematic viscosity [$m^2{\cdot}s^{-1}$]
$\overline{Nu_D}$	Nusselt number [dimensionless]
Pr	Prandtl number [dimensionless]
Ra_D	Rayleigh number [dimensionless]

References

Abanikannda, O.T.F., Olutogun, O., Leigh, A.O., Ajayi, L.A., 2007. Statistical modeling of egg weight and egg dimensions in commercial layers. Int J Poult Sci 6 (1), 59–63.

Abbasnezhad, B., Hamdami, N., Khodaei, D., 2015. Modeling of rheological characteristics of liquid egg white and yolk at different pasteurization temperatures. J. Food Meas. Char. 9 (3), 359–368. https://doi.org/10.1007/s11694-015-9243-6.

Abbasnezhad, B., Hamdami, N., Monteau, J.Y., Vatankhah, H., 2016. Numerical modeling of heat transfer and pasteurizing value during thermal processing of intact egg. Food Sci. Nutr. 4 (1), 42–49. https://doi.org/10.1002/fsn3.257.

Agregán, R., et al., 2023. The use of novel technologies in egg processing. Food Rev. Int. 39 (5), 2854–2874. https://doi.org/10.1080/87559129.2021.1980887.

Atilgan, M.R., Unluturk, S., 2008. Rheological properties of liquid egg products (LEPS). Int. J. Food Prop. 11 (2), 296–309. https://doi.org/10.1080/10942910701329658.

Bermudez-Aguirre, D., Niemira, B.A., 2023. A review on egg pasteurization and disinfection: Traditional and novel processing technologies. John Wiley and Sons Inc. https://doi.org/10.1111/1541-4337.13088.

Chantarapanont, W., Slutsker, L., V Tauxe, R., Beuchat, L.R., 2000. Factors influencing inactivation of salmonella enteritidis in hard-cooked eggs.

Chhanwal, N., Tank, A., Raghavarao, K.S.M.S., Anandharamakrishnan, C., 2012. Computational fluid dynamics (CFD) modeling for bread baking process-a review. Food Bioproc Tech 5 (4), 1157–1172. https://doi.org/10.1007/s11947-012-0804-y.

Coimbra, J.S.R., Gabas, A.L., Minim, L.A., Garcia Rojas, E.E., Telis, V.R.N., Telis-Romero, J., 2006. Density, heat capacity and thermal conductivity of liquid egg products. J. Food Eng. 74 (2), 186–190. https://doi.org/10.1016/j.jfoodeng.2005.01.043.

Davari, M., Bahreini, M., Sabzevari, Z., 2024. Developing a non-destructive method for the detection of egg quality and freshness using micro-Raman spectroscopy. Applied Food Research 4 (2). https://doi.org/10.1016/j.afres.2024.100453.

Denys, S., Pieters, J.G., Dewettinck, K., 2003. Combined CFD and experimental approach for determination of the surface heat transfer coefficient during thermal processing of eggs. J. Food Sci. 68 (3), 943–951.

Denys, S., Pieters, J.G., Dewettinck, K., 2004. Computational fluid dynamics analysis of combined conductive and convective heat transfer in model eggs. J. Food Eng. 63 (3), 281–290. https://doi.org/10.1016/j.jfoodeng.2003.06.002.

Denys, S., Pieters, J.G., Dewettinck, K., 2005. Computational fluid dynamics analysis for process impact assessment during thermal pasteurization of intact eggs. J Food Prot 68 (2), 366–374.

Ferry, J.D., 1948. Protein gels. Adv. Protein Chem. 4, 1–78.

Galante, M., et al., 2011. Eggstraordinary eggsperiments an activity to teach heat transfer concepts to K-12 students. Ann Arbor, [Online]. Available: http://www-personal.umich.edu/~ajyshih/egg/Eggsperiment/Home.html.

Grijspeerdt, K., Herman, L., 2003. Inactivation of salmonella enteritidis during boiling of eggs. Int. J. Food Microbiol. 82, 13–24 [Online]. Available: www.elsevier.com/locate/ijfoodmicro.

Grunden, L.P., Mulnix, E.J., Darfler, J.M., Baker, R.C., 1975. Yolk position in hard cooked eggs as related. Poult Sci 54, 546–552.

Gut, J.A.W., et al., 2003. Pasteurization of egg Yolk in plate heat exchangers: thermophysical properties and process simulation.

He, J., Wong, C.W.Y., Schultze, D.M., Wang, S., 2024. Inactivation of salmonella enteritidis in liquid egg yolk and egg white using bacteriophage cocktails. Curr. Res. Food Sci. 8 (Jan). https://doi.org/10.1016/j.crfs.2024.100703.

Iannotti, L.L., Lutter, C.K., Bunn, D.A., Stewart, C.P., 2014. Eggs: the uncracked potential for improving maternal and young child nutrition among the world's poor. Nutr. Rev. 72 (6), 355–368. https://doi.org/10.1111/nure.12107.

Jenko, M., 2015. Numerical cooking for pasteurized soft boiled eggs. Strojniski Vestnik/Journal of Mechanical Engineering 61 (5), 319–329. https://doi.org/10.5545/sv-jme.2014.2187.

Jiang, J., et al., 2024. Regulating the thermal properties of egg white by adding surfactants. J. Food Eng. 362 (Feb). https://doi.org/10.1016/j.jfoodeng.2023.111759.

Khan, M.I.H., Joardder, M.U.H., Kumar, C., Karim, M.A., 2018. Multiphase porous media modelling: A novel approach to predicting food processing performance. Crit. Rev. Food Sci. Nutr. 58 (4), 528–546. https://doi.org/10.1080/10408398.2016.1197881.

Kruenti, F., Hagan, J.K., Ansong, M.O., Lamptey, V.K., 2022. The quality of white and brown chicken eggs kept under different storage length and storage temperatures. Journal of Innovative Agriculture 9 (2), 1–11. https://doi.org/10.37446/jinagri/rsa/9.2.2022.1-11.

Kumar, V., Jonnalagadda, D., Subbiah, J., Wee, A.P., Thippareddi, H., Birla, S., 2009. A 3-D heat transfer and fluid flow model for cooling of a single egg under forced convection. Trans. ASABE (Am. Soc. Agric. Biol. Eng.) 52 (5), 1627–1637.

Kumar, V., Wee, A.P., Birla, S., Subbiah, J., Thippareddi, H., 2012. A 3-D computational fluid dynamics model for forced air cooling of eggs placed in trays. J. Food Eng. 108 (3), 480–492. https://doi.org/10.1016/j.jfoodeng.2011.08.003.

Liu, L., Xie, T., Cheng, W., Ding, Y., Xu, B., 2024. Characterization and mechanism of thermally induced tea polyphenols and egg white proteins gel system and its 3D printing. LWT 205 (Aug). https://doi.org/10.1016/j.lwt.2024.116488.

Llave, Y., Fukuda, S., Fukuoka, M., Shibata-Ishiwatari, N., Sakai, N., 2018. Analysis of color changes in chicken egg yolks and whites based on degree of thermal protein

denaturation during ohmic heating and water bath treatment. J. Food Eng. 222, 151–161. https://doi.org/10.1016/j.jfoodeng.2017.11.024.
Luo, X., et al., 2024. Effects of different temperatures on the physicochemical characteristics, microstructure and protein structure of preserved egg yolk. Food Chem. X 22 (Jun). https://doi.org/10.1016/j.fochx.2024.101278.
Melo, E.F., Araújo, I.C.S., Triginelli, M.V., Castro, F.L.S., Baião, N.C., Lara, L.J.C., 2021. Effect of egg storage duration and egg turning during storage on egg quality and hatching of broiler hatching eggs. Animal 15 (2). https://doi.org/10.1016/j.animal.2020.100111.
Minéia, C., De Paula, D., Fogliatto, R., And, M., Tondo, E.C., 2005. Thermal inactivation of salmonella enteritidis by boiling and frying egg methods. J. Food Saf. 25, 43–57.
Morris, S.S., Beesabathuni, K., Headey, D., 2018. An egg for everyone: pathways to universal access to one of nature's most nutritious foods. Matern. Child Nutr. 14. https://doi.org/10.1111/mcn.12679.
Moukalled, F., Mangani, L., Darwish, M., 2016. The Finite Volume Method in Computational Fluid Dynamics. Springer [Online]. Available: http://www.springer.com/series/5980.
Nellis, Gregory, Klein, S.A., 2009. Heat Transfer. Cambridge University Press.
Ogura, T., et al., 2020. Effects of feed crops and boiling on chicken egg yolk and white determined by a metabolome analysis. Food Chem. 327. https://doi.org/10.1016/j.foodchem.2020.127077.
Omar, Mohamad Fithri Akmar, et al., 2018. Determination of the optimum time for preparation of half-boiled eggs free from salmonella enterica serovar enteritidis. Journal of Clinical and Heatlh Sciencies 3 (1), 16–19.
Pero, M., Kiani, H., Askari, G., 2019. A novel numerical approach for modeling the coagulation phenomenon in egg white. J. Food Process. Eng. 42 (4). https://doi.org/10.1111/jfpe.13033.
Ramachandran, R., Malhotra, D., Anishaparvin, A., Anandharamakrishnan, C., 2011. Computational fluid dynamics simulation studies on pasteurization of egg in stationary and rotation modes. Innovative Food Sci. Emerging Technol. 12 (1), 38–44. https://doi.org/10.1016/j.ifset.2010.11.008.
Razi, S.M., Fahim, H., Amirabadi, S., Rashidinejad, A., 2023. An Overview of the Functional Properties of Egg White Proteins and Their application in the food industry. Elsevier B.V. https://doi.org/10.1016/j.foodhyd.2022.108183
Rodríguez Maestre, I., Gómez Sánchez, J.J., González Gallero, F.J., Foncubierta Blázquez, J.L., 2021. Performance analysis of natural convection correlations for spheres at high Rayleigh numbers. Int. J. Therm. Sci. 168. https://doi.org/10.1016/j.ijthermalsci.2021.107061.
Rossi, M., Schiraldi, A., 1992. Thermal denaturation and aggregation of egg proteins. Thermochim. Acta 199, 115–123.
Shahbaz, H.M., et al., 2018. Application of high pressure processing for prevention of greenish-gray yolks and improvement of safety and shelf-life of hard-cooked peeled eggs. Innovative Food Sci. Emerging Technol. 45, 10–17. https://doi.org/10.1016/j.ifset.2017.09.016.
Szpicer, A., Binkowska, W., Stelmasiak, A., Wojtasik-Kalinowska, I., Wierzbicka, A., Poltorak, A., 2023a. Application of computational fluid dynamics simulation in predicting food protein denaturation: numerical studies on selected food products - a review. Anim. Sci. Pap. Rep. 41 (4), 307–332. https://doi.org/10.2478/aspr-2023-0014.
Szpicer, A., Bińkowska, W., Wojtasik-Kalinowska, I., Salih, S.M., Półtorak, A., 2023b. Application of computational fluid dynamics simulations in food industry. European Food Research and Technology 249 (6), 1411–1430. https://doi.org/10.1007/s00217-023-04231-y.
Szpicer, A., Binkowska, W., Wojtasik-Kalinowska, I., Poltorak, A., 2023c. Prediction of protein denaturation and weight loss in pork loin (muscle Longissimus dorsi) using computational fluid dynamics. European Food Research and Technology 249 (12), 3055–3068. https://doi.org/10.1007/s00217-023-04348-0.
Wang, C., Llave, Y., Sakai, N., Fukuoka, M., 2021. Analysis of thermal processing of liquid eggs using a high frequency ohmic heating: experimental and computer simulation approaches. Innovative Food Sci. Emerging Technol. 73 (Oct). https://doi.org/10.1016/j.ifset.2021.102792.
Wang, C., Llave, Y., Fukuoka, M., 2024. Agitation of liquid eggs during ohmic heating pasteurization—experimental and computer simulation study. J. Food Process. Eng. 47 (1). https://doi.org/10.1111/jfpe.14541.
Wu, C.C., Völker, D., Weisbrich, S., Neitzel, F., 2022. The finite volume method in the context of the finite element method. In: Materials Today: Proceedings. Elsevier Ltd, pp. 2679–2683. https://doi.org/10.1016/j.matpr.2022.05.460.
Yamak, U.S., Sarica, M., Boz, M.A., Ucar, A., 2016. The effect of eggshell thickness on hatching traits of partridges. Rev. Bras. Ciência Avícola/Brazilian Journal of Poultry Science 18 (SpecialIssue), 13–17. https://doi.org/10.1590/1806-9061-2015-0039.